Biochimica et Biophysica Acta 1797 (2010) 557–565

Contents lists available at ScienceDirect

Biochimica et Biophysica Acta

journal homepage: www.elsevier.com/locate/bbabio

Kinetic model of the inhibition of respiration by endogenous nitric oxide in intact cells

Enara Aguirre [a,1], Félix Rodríguez-Juárez [a,1], Andrea Bellelli [b], Erich Gnaiger [c], Susana Cadenas [a,d,*]

[a] Department of Regenerative Cardiology, Centro Nacional de Investigaciones Cardiovasculares (CNIC), Melchor Fenández Almagro 3, 28029 Madrid, Spain
[b] Dipartimento di Scienze Biochimiche and Istituto di Biologia e Patologia Molecolari del CNR, Università di Roma 'Sapienza', 00185 Roma, Italy
[c] Department of General and Transplant Surgery, D. Swarovski Research Laboratory, Medical University of Innsbruck, 6020 Innsbruck, Austria
[d] Servicio de Inmunología, Hospital Universitario de La Princesa, Diego de León 62, 28006 Madrid, Spain

ARTICLE INFO

Article history:
Received 28 July 2009
Received in revised form 25 January 2010
Accepted 27 January 2010
Available online 6 February 2010

Keywords:
Nitric oxide
Mitochondrial respiration
Cytochrome *c* oxidase
Oxygen consumption
Mitochondria
Kinetic model

ABSTRACT

Nitric oxide (NO) inhibits mitochondrial respiration by decreasing the apparent affinity of cytochrome *c* oxidase (CcO) for oxygen. Using iNOS-transfected HEK 293 cells to achieve regulated intracellular NO production, we determined NO and O_2 concentrations and mitochondrial O_2 consumption by high-resolution respirometry over a range of O_2 concentrations down to nanomolar. Inhibition of respiration by NO was reversible, and complete NO removal recovered cell respiration above its routine reference values. Respiration was observed even at high NO concentrations, and the dependence of IC_{50} on [O_2] exhibits a characteristic but puzzling parabolic shape; both these features imply that CcO is protected from complete inactivation by NO and are likely to be physiologically relevant. We present a kinetic model of CcO inhibition by NO that efficiently predicts experimentally determined respiration at physiological O_2 and NO concentrations and under hypoxia, and accurately predicts the respiratory responses under hyperoxia. The model invokes competitive and uncompetitive inhibition by binding of NO to the reduced and oxidized forms of CcO, respectively, and suggests that dissociation of NO from reduced CcO may involve its O_2-dependent oxidation. It also explains the non-linear dependence of IC_{50} on O_2 concentration, and the hyperbolic increase of c_{50} as a function of NO concentration.

1. Introduction

Nitric oxide (NO) is a fundamental cell messenger produced in cells by NO synthases (NOS). Many physiological actions of NO are mediated through activation of soluble guanylate cyclase and subsequent production of cGMP [1,2]. NO is also an effective inhibitor of mitochondrial respiration [3–5]: it reversibly inhibits cytochrome *c* oxidase (CcO), the terminal electron acceptor of the mitochondrial respiratory system, in a process which occurs in competition with oxygen (O_2). NO, like other inhibitors that raise the K'_m of CcO, induces O_2 limitation under apparently normoxic conditions. The inhibition of mitochondrial respiration by NO has been implicated in a wide range of physiological processes, including the regulation of the affinity of mitochondrial respiration for O_2 [6–10], the control of mitochondrial generation of superoxide [11] and hydrogen peroxide [12], the activation of hypoxia-inducible factor [13], the activation of AMPK in astrocytes [14], the modulation of O_2 delivery to tissues [15], the modulation of calcium-mediated cell signaling in the brain [16] and the maintenance of constant cerebral O_2 consumption at varying blood flow [17]. The interaction between CcO and NO has been implicated in various pathophysiological situations [18,19].

The molecular mechanism by which NO inhibits CcO has not been fully defined (for a review see [20]). The enzyme belongs to the superfamily of heme-copper oxidases and contains a highly conserved bimetallic active site composed of a high-spin heme a_3 and a copper ion Cu_B. The binuclear center is the binding site of the physiological substrate O_2 and of other ligands such as CN^-, CO, and NO [21]. O_2-binding demands the complete reduction of the active site: two electrons donated by cytochrome *c* enter CcO at Cu_A, from which they are transferred, via cytochrome *a*, to the binuclear center. Conflicting hypotheses have been proposed to explain the mechanism of CcO inhibition by NO [22–24]; however, recent studies demonstrate that NO interactions with CcO cannot be adequately described by a simple competitive model and that only one NO molecule binds per binuclear center [25]. The enzyme can bind NO either at the reduced heme a_3 iron (competitive with O_2) or at the oxidized Cu_B (non-competitive with O_2)

Abbreviations: NO, nitric oxide; NOS, NO synthase; CcO, cytochrome *c* oxidase; O_2, oxygen; CN^-, cyanide; CO, carbon monoxide; iNOS, inducible NOS; DMEM, Dulbecco's modified Eagle's medium; Tet-iNOS 293, tetracycline-inducible iNOS-expressing HEK 293 cells; S-EITU, S-ethylisothiourea; FCCP, carbonylcyanide *p*-(trifluoromethoxy) phenylhydrazone; HBSS, Hanks balanced salt solution; HbO_2, oxyhemoglobin

* Corresponding author. Servicio de Inmunología, Hospital Universitario de La Princesa, Diego de León 62, 28006 Madrid, Spain. Tel.: +34 915202386; fax: +34 915202374.
E-mail address: susana.cadenas@salud.madrid.org (S. Cadenas).

[1] These authors contributed equally to this work.

0005-2728/$ – see front matter © 2010 Elsevier B.V. All rights reserved.
doi:10.1016/j.bbabio.2010.01.033

[25–28]. NO binds to reduced heme a_3 very quickly and with high affinity, to yield a Fe^{2+}-NO nitrosyl-adduct. Through binding to oxidized Cu_B, donation of an electron to the metal and subsequent hydration, NO is oxidized to nitrite. The predominance of one inhibitory mechanism over the other is controlled by the electron flux through the enzyme [29]. NO and its derivative peroxynitrite have also been reported to irreversibly decrease the affinity of CcO for O_2 [30], although this effect is unlikely to occur at physiological NO levels.

The complexity of the cellular environment provides the ideal setting for studying how the interplay between O_2 and NO concentrations determines the extent of respiratory inhibition and the O_2-dependence of iNOS-mediated NO production. However, because of technical limitations, previous studies have not provided accurate kinetic data at low [O_2]. Additionally, in many studies sensitivity of O_2 consumption to NO donors has been examined at [O_2] much higher than those likely to exist *in vivo*. High-resolution respirometry allows accurate determination of respiration at low O_2 concentrations and during transition to anoxia [31]. Here we present a detailed study of the O_2 kinetics of cellular respiration in intact cells producing controlled amounts of NO [32]. Insertion of an NO sensor into the Oxygraph-2k respirometer chamber allowed simultaneous recording of NO production and mitochondrial respiration over an extended [O_2] range. Based on our results, we present a pseudo-equilibrium kinetic model of inhibition of respiration by NO that accounts for both competitive and uncompetitive inhibition of CcO and has predictive value.

2. Materials and methods

2.1. Cell culture and reagents

Tetracycline-inducible HEK 293 cells stably expressing human iNOS (Tet-iNOS 293) were generated as described [32]. Cells were cultured in DMEM (Invitrogen, Barcelona, Spain) containing 4.5 g/l D-glucose, 10% (v/v) fetal-calf serum, 200 μg/ml hygromycin B and 15 μg/ml blasticidin, at 37 °C in a humidified atmosphere with 5% CO_2. S-ethylisothiourea hydrobromide (S-EITU; NOS inhibitor), L-arginine, oligomycin and FCCP were from Sigma-Aldrich (St. Louis, MO). Hygromycin B and blasticidin were from Invitrogen. Tetracycline was from Calbiochem (Darmstadt, Germany).

2.2. Induction of endogenous NO production

Expression of iNOS was induced as previously described [33]. Briefly, cells were incubated overnight in a complete growth medium (without selection antibiotics) containing tetracycline (5–50 ng/ml) and 500 μM S-EITU, a potent inhibitor of iNOS activity. Cells were washed with L-arginine-free DMEM supplemented with 1% dialysed fetal-calf serum to eliminate any traces of L-arginine. Cells were incubated in L-arginine-free medium for 1 h to completely eliminate S-EITU and tetracycline without activating NO production. Cells were trypsinized and resuspended at 1×10^7 cells/ml in HBSS containing 25 mM Hepes. Endogenous NO production was triggered by addition of L-arginine (1 mM).

2.3. Immunoblot analysis of iNOS expression

For preparation of total protein extracts, cells were trypsinized and resuspended at 1×10^7 cells/ml in HBSS containing 25 mM Hepes. Cells were spun (300 *g*, 5 min, 4 °C) and the pellet was resuspended in 60 μl ice-cold lysis buffer (20 mM Hepes, pH 7.5, 400 mM NaCl, 20% (v/v) glycerol, 0.1 mM EDTA, 10 mM NaF, 10 μM Na_2MoO_4, 1 mM $NaVO_3$, 10 mM PNPP (*p*-nitrophenyl phosphate), and 10 mM β-glycerophosphate) supplemented with 1 mM dithiothreitol, 1 mM pefablock, pH 7.4, and a protease-inhibitor cocktail (Roche Diagnostics, Barcelona, Spain). After 15 min on ice, cleared whole cell extracts were obtained by recovering the supernatant after centrifugation (16,000 *g*, 15 min, 4 °C). Protein samples (200 μg) were resolved by SDS/7.5%-(w/v)-PAGE and transferred to nitrocellulose membranes. Membranes were blocked with 5% (w/v) non-fat dry milk in TBS-T (20 mM Tris/HCl, pH 7.2, 150 mM NaCl, 0.1% Tween 20) and incubated overnight with polyclonal anti-iNOS antibody (1:2000, Transduction Laboratories, Erembodegem, Belgium) in a blocking solution at 4 °C. Protein bands were detected by incubation for 1 h with horseradish peroxidase-coupled goat anti-rabbit IgG (1:5000; Vector Laboratories, Burlingame, CA) in blocking solution at room temperature, followed by enhanced chemiluminescence (GE Healthcare, Amersham, UK).

2.4. Simultaneous measurement of O_2 consumption and NO production

O_2 consumption at physiological tissue [O_2] was determined by high-resolution respirometry (Oxygraph-2k; Oroboros Instruments, Innsbruck, Austria). Cells were trypsinized after overnight treatment with tetracycline and resuspended in HBSS containing 25 mM Hepes at 1×10^7 cells/ml. The instrumental background flux was calculated as a linear function of [O_2] and the experimental data were corrected for the whole range of [O_2] using DatLab software (Oroboros Instruments) [31]. To separate mitochondrial and residual O_2 consumption, all results were corrected for residual O_2 consumption of 0.5 pmol $O_2 \cdot s^{-1} \cdot 10^{-6}$ cells, measured at 35 μM O_2 (Table 1). Compared with CcO, residual oxygen uptake has a lower affinity for oxygen [34]. This was accounted for by assigning a 5-fold higher c_{50} to residual respiration as a basis for application of the residual O_2 consumption–correction over the entire experimental [O_2] range. At air saturation, 37 °C and local barometric pressure (92.6 kPa), the [O_2] in culture medium (HBSS) was 175.7 μM (O_2 solubility factor 0.92). Measurements were taken in cell suspensions (2 ml) gently agitated at 37 °C in parallel Oxygraph-2k chambers; NO production was initiated in one chamber by addition of 1 mM L-arginine; a control run (in cells treated with the same amount of tetracycline) was simultaneously performed in the other chamber. Because light reverses NO-induced inhibition of respiration [35–37] O_2 consumption was measured in the dark, except for analysis of inhibition reversibility, when cell suspensions were illuminated with cold light (Intralux 5000-1; Volpi, Switzerland). Reversibility was also studied by adding HbO_2 to quench NO or S-EITU (1 mM) to inhibit iNOS activity.

For the simultaneous measurement of endogenous NO production, an NO sensor (ISO-NOP; World Precision Instruments, Stevenage, UK) was inserted into the Oxygraph-2k chamber. For this, a second capillary was drilled into the PVDF stopper to tightly fit the 2 mm diameter sleeve of the NO sensor. The opening of the second capillary did not increase O_2 backdiffusion into the chamber at low [O_2]. The NO sensor was calibrated by addition of known $NaNO_2$ concentrations under reducing conditions (KI/H_2SO_4) at 37 °C. To initiate NO production, 1 mM L-arginine was added to the chamber at 60 μM O_2. This [O_2] is sufficient to sustain iNOS activity [38,39]. NO concentrations were monitored until O_2 was exhausted and the NO signal returned to basal. The NO signal

Table 1
Routine respiration, electron transport capacity, and resting and residual respiration in Tet-iNOS 293 cells. Respiration of control cells in the absence of NO (cells were not treated with tetracycline and no arginine was added). Routine: basal respiration using endogenous substrates. Resting: addition of oligomycin (80 ng/ml) to measure respiration in the absence of ATP synthesis. Uncoupled: addition of optimum FCCP concentration (0.35 μM) for maximum flow to measure the capacity of the electron transport system. Corrections were made for residual O_2 consumption (1 mM KCN at 30 to 40 μM O_2). Measurements were made at 37 °C at 1×10^7 cells/ml in the chambers of a high-resolution respirometer. Values are means ± SD (number of independent experiments in parentheses).

Respiratory state endogenous substrates	Respiration [pmol $O_2 \cdot s^{-1} \cdot 10^{-6}$ cells]	Flux control ratio per uncoupled rate
Routine	14.5 ± 1.9 (8)	0.31 ± 0.03
Resting (oligomycin)	4.2 ± 0.4 (3)	0.089 ± 0.004
Uncoupled (FCCP)	47.4 ± 7.1 (8)	
Residual (KCN)	0.51 ± 0.08 (5)	0.011 ± 0.003

before addition of L-arginine was used for internal zero calibration, and non-linear zero drift was observed before addition of L-arginine and after zero O_2 was reached. A polynomial interpolation of these sections of the zero signal was used to construct a zero-baseline, which was subtracted from the total signal.

2.5. Data analysis

Data were analyzed by standard least squares non-linear minimization routines, written with the Matlab program (MathWorks, Natick, MA).

3. Results

3.1. Routine, uncoupled and oligomycin-inhibited respiration

Cell respiration was measured in intact Tet-iNOS 293 cells, which express iNOS upon treatment with tetracycline [32] (Fig. 2E). Cell respiration with endogenous substrates was determined in cells not expressing iNOS, suspended in HBSS containing 25 mM Hepes. Routine O_2 consumption was 14.5 ± 1.9 pmol $O_2 \cdot s^{-1} \cdot 10^{-6}$ cells, corrected for residual O_2 consumption after inhibition of CcO. Uncoupled respiration was three-fold higher than routine respiration (Table 1), indicating that endogenous respiration has a large potential for activation and is not substrate-limited. Upon addition of oligomycin to inhibit ATP synthase, respiration declined to around 10% of uncoupled or 30% of routine respiration, showing that a high proportion of routine respiration is coupled to ATP synthesis. Residual O_2 consumption, measured after addition of 1 mM KCN to inhibit CcO, was as low as 3% of routine respiration.

3.2. O_2 kinetics in the absence of NO

In the absence of NO, routine respiration followed a strictly hyperbolic function, fitted in the low-O_2 range (<11 μM; Fig. 1A and B). The [O_2] at half-maximum flux, c_{50} (equivalent to the apparent $K_{m,O2}$) [40], was 0.65 μM ± 0.04 SD ($n = 5$) for routine respiration in control cells (not expressing iNOS) and was unaffected by addition of 1 mM L-arginine (Fig. 1A and B). The c_{50} agrees with the results obtained in human umbilical vein endothelial cells [41] and fibroblasts [42], and is comparable to the c_{50} in isolated mitochondria [40,43].

3.3. Endogenous NO production and inhibition of respiration by NO in the low-O_2 range

Overnight incubation of cells with increasing concentrations of tetracycline (10–50 ng/ml) induced a concentration-dependent expression of iNOS, as determined by western blot (Fig. 2E). Addition of the iNOS substrate L-arginine (1 mM) at 60 μM O_2 immediately triggered NO production, as shown by a steady increase of [NO] (Fig. 1C). The amount of NO produced by cells after addition of L-arginine was proportional to the level of iNOS expression. In the physiological O_2 range, even low [NO] (30 nM) caused a significant right-shift in the O_2 kinetics of cell respiration (Fig. 1D; compare with Fig. 1B). When [O_2] had dropped to ~15 μM, NO degradation balanced NO production. iNOS activity is progressively limited as [O_2] decreases (iNOS has a high K_m for O_2; [38,39]). At low [O_2], however, mitochondria are capable of producing NO from

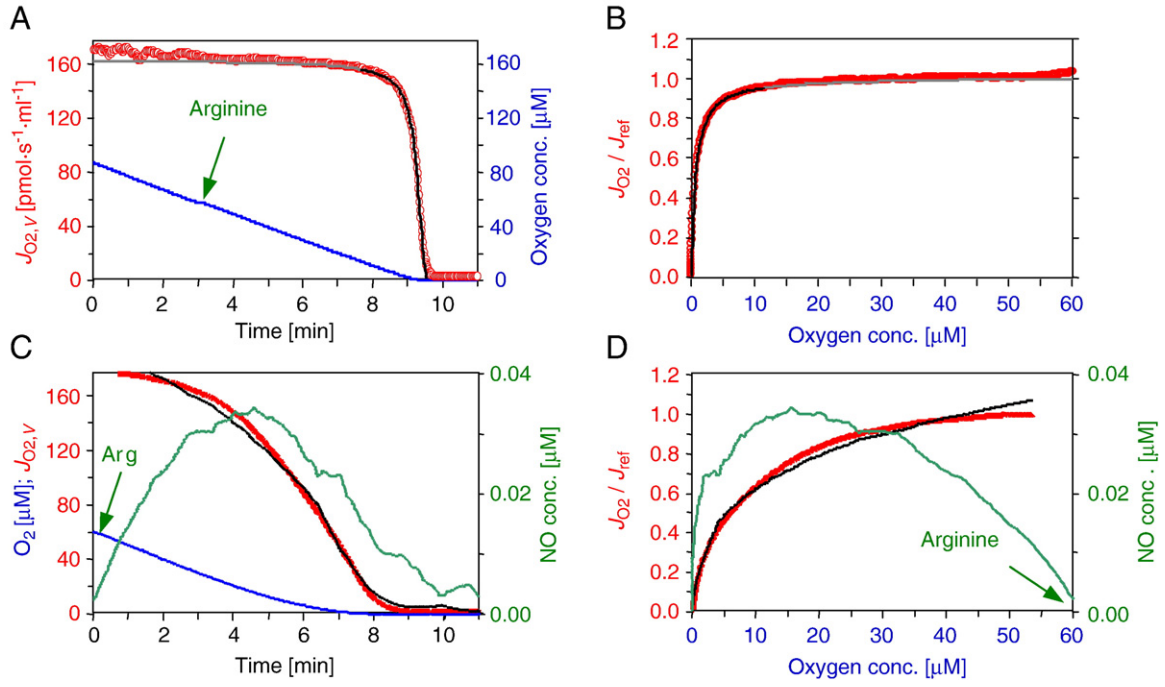

Fig. 1. Cell respiration in the absence or presence of low levels of NO production. O_2 consumption and NO production were measured in cells without (A,B) and with (C,D) iNOS induction (20 ng/ml tetracycline). (A,C) Oxygraph-2k traces of [O_2] (blue), O_2 flux (red) and [NO] (green) as a function of time, with data points plotted at 1 s intervals. (B,D) Kinetic plots of O_2 flux as a function of [O_2] in the low-O_2 range (<11 μM). (A,B) The hyperbolic fits (black) almost perfectly superimpose the measured data points. (D) The graph shows relative measured flux (red) calculated relative to routine flux recorded at saturating [O_2] (J_{ref}), relative calculated flux from the kinetic model (black), and [NO] (green) as a function of [O_2] at low levels of NO production (20 ng/ml tetracycline).

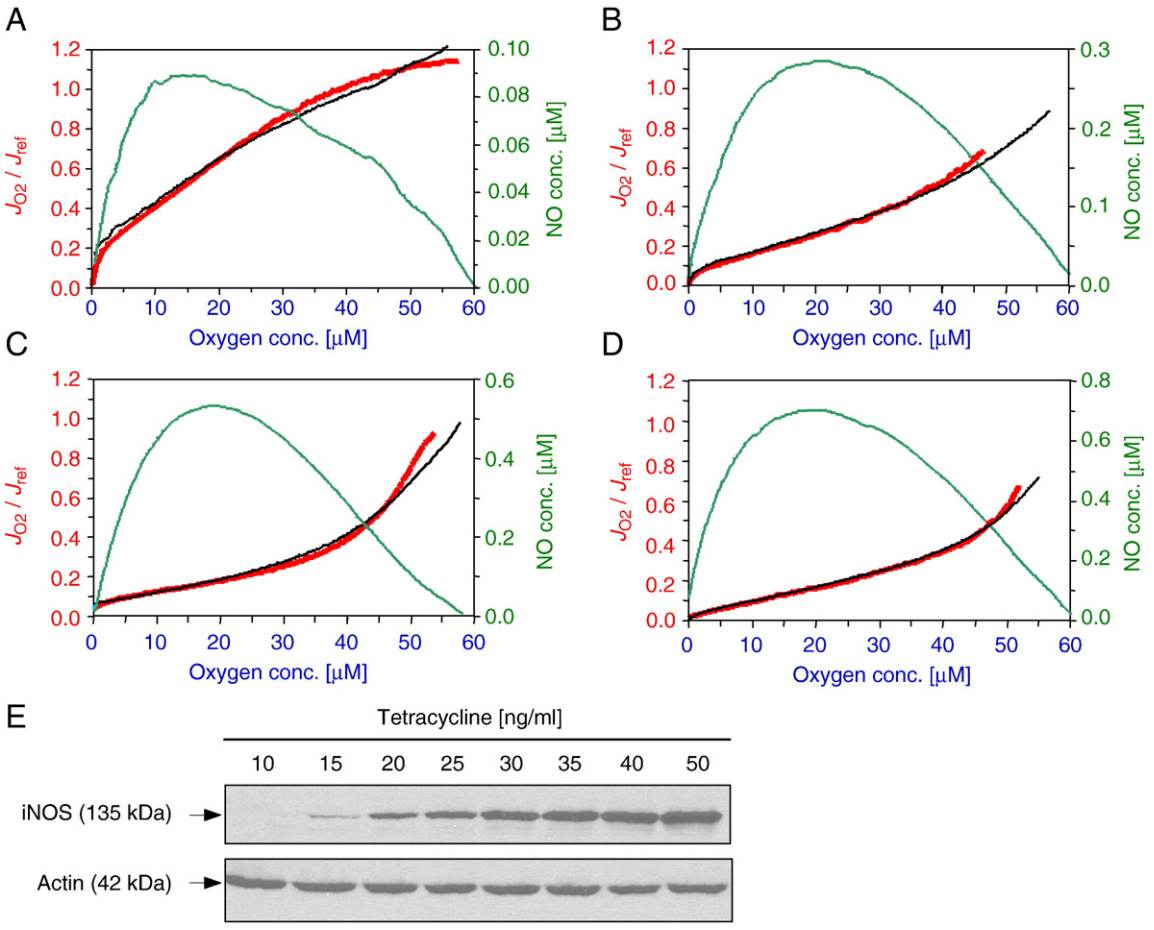

Fig. 2. Endogenous NO production and NO-induced inhibition of cell respiration. (A–D) Kinetic plots of O_2 flux as a function of [O_2] in the low-O_2 range (<11 μM), and electrochemical measurement of NO, in cells with iNOS induction. The graphs show relative measured flux (red) calculated relative to routine flux recorded at saturating [O_2] (J_{ref}), relative calculated flux from the kinetic model (black), and [NO] (green) as a function of [O_2] at three levels of NO production: (A) low production (20 ng/ml tetracycline); (B,C) intermediate production (25 ng/ml tetracycline), and (D) high production (30 ng/ml tetracycline). Traces are representative of five similar experiments. (E) Western blot showing the expression of iNOS after overnight induction with tetracycline (10–50 ng/ml). Expression of actin was detected as a loading control.

nitrite (NO_2^-) [44]. [NO] declined to zero when O_2 was exhausted by cell respiration (Fig. 1C and D). Accordingly, addition of L-arginine at zero [O_2] did not induce detectable NO production (not shown).

The rate of NO production and the maximum [NO] obtained in the experimental low-O_2 regime were a function of iNOS expression (Fig. 1C and D; Fig. 2A–D). For each experiment, the reference flux (J_{ref}), corresponding to routine respiration, was measured when [O_2] was not limiting and before addition of L-arginine. Respiration was inhibited as a complex function of O_2-dependent NO production and O_2 limitation of CcO (Fig. 1D; Fig. 2A–D). Two experimental observations were particularly puzzling. First, CcO maintained residual activity up to 2 μM NO even at [O_2] in the low μM range, in spite of the fact that CcO inhibition was already detectable at low-nM [NO] (see Fig. 2D; Fig. 5B and D). This cannot be explained by O_2 consumption by other enzyme systems and suggests that at least one NO-bound derivative of CcO is active and reduces O_2. Second, the [NO] required to inhibit CcO by 50% at any given [O_2] (IC_{50}) has an unusual parabolic dependence on [O_2] (Fig. 3B; see also [24]). A similar upward parabolic trend was obtained when NO was generated from the NO donor DETA-NONOate (Fig. S1).

The interdependence of NO and O_2 concentrations generally makes it impossible to apply kinetic fitting procedures that depend on variation of substrate (O_2) concentration at a constant concentration of the inhibitor (NO). We therefore applied an approach in which kinetic parameters were fitted to all data points of all experiments simultaneously.

3.4. Kinetic model of CcO inhibition by NO

Consistent with previous observations [25–28], our data cannot be adequately explained by a simple competitive inhibition model in which NO binds to the reduced heme a_3 of CcO in place of O_2, especially in relation to the residual activity at high [NO] and the dependence of IC_{50} on [O_2]. These perplexing features would be explained if CcO catalyzed oxidation of NO, at least under some experimental conditions. We therefore tested two minimal chemically-sound, albeit oversimplified, models that allow NO to be oxidized by O_2. One considers oxidation of NO bound to the reduced heme a_3; the other, oxidation of NO bound to the oxidized Cu_B. Although both models were comparably successful, only the first is described here (see Fig. 4), since it has better independent support [45,46]. In this model, when NO occupies the heme a_3, effectively competing with O_2, an alternative catalytic pathway is opened, whereby O_2 transiently binds to reduced Cu_B, is activated to superoxide and is forced to react with NO to yield peroxynitrite, which spontaneously converts to nitrite (NO_2^-) [46].

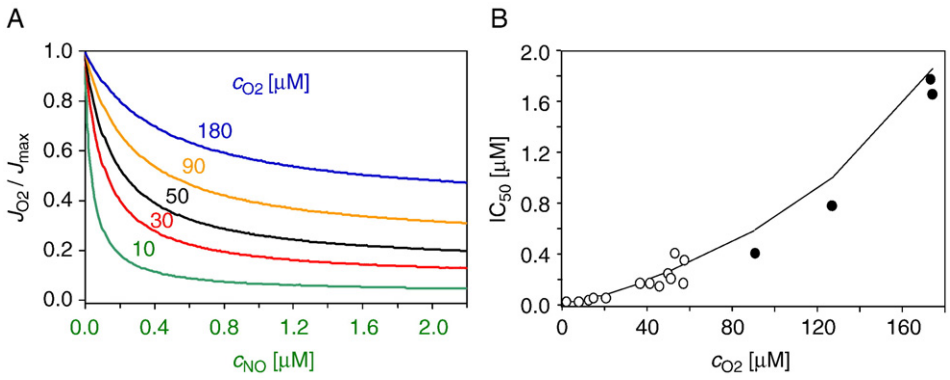

Fig. 3. Relationship between NO concentration and the degree of inhibition of respiration. (A) Effect of [NO] on the relative O_2 flux, calculated from the kinetic parameters at constant [O_2] of 10 μM (green), 30 μM (red), 50 μM (black), 90 μM (yellow), or 180 μM (blue). (B) IC_{50} (μM) as a function of [O_2]; open symbols are from experiments carried out in the low [O_2] range; closed symbols from the high [O_2] range. The line is drawn according to Eq. (4), using the parameters reported in the text.

In the model, both reduced species, CcO_rNO and CcO_r, are catalytically active. The sum of the enzyme intermediates predicted at any given concentrations of O_2 and NO is given by the following partition function:

$$[CcO_{tot}] = [CcO_r](1 + [O_2]/K_{m1} + [NO]/K_{icNO} + [O_2][NO]/K_{m2}K_{icNO} + [O_2][NO]/K_{uNO}K_{m1}) \quad (1)$$

where CcO_{tot} is the total (all species) CcO; CcO_r is the reduced CcO; K_{m1} is the K_m of CcO for O_2 in the absence of NO; K_{m2} is the K_m of CcO for O_2 when NO is bound to heme a_3; K_{icNO} is the competitive inhibition constant of NO for CcO, and K_{uNO} is the uncompetitive inhibition constant of NO for CcO.

The rate of respiration is described by Eq. (2):

$$V = \frac{[CcO_{tot}]V_{max1}([O_2]K_{uNO}K_{m2}K_{icNO} + r[O_2][NO]K_{m1}K_{uNO})}{K_{m1}K_{m2}K_{icNO}K_{uNO} + [O_2]K_{m2}K_{icNO}K_{uNO} + [O_2][NO]K_{m2}K_{icNO} + [NO]K_{m1}K_{m2}K_{uNO} + [O_2][NO]K_{m1}K_{uNO}} \quad (2)$$

where r represents the ratio V_{max2}/V_{max1} (which we estimate at ~1.35). Notice that the oxidative dissociation of NO bound to Cu_B as nitrite ion governed by V_{NO} (see Fig. 4) does not involve O_2 consumption and therefore does not appear in Eq. (2).

Analysis by standard least squares non-linear minimization routines yielded the following parameter values: $K_{m1} = 0.81$ μM, $V_{max1} = 16.5$ pmol $O_2 \cdot s^{-1} \cdot 10^{-6}$ cells, $K_{icNO} = 3.63$ nM, $K_{m2} = 520$ μM and $V_{max2} = 22$ pmol $O_2 \cdot s^{-1} \cdot 10^{-6}$ cells. K_{uNO} was higher than the usual NO concentrations achieved in this study, thus it was poorly determined and could be dropped from the fit. The best fit to the experimental data requires the affinity of O_2 for CcO to be modulated by enzyme-bound NO, such that the species CcO_rNO (with NO bound to heme a_3) has a higher K_m for O_2 (K_{m2}) than the uninhibited enzyme (K_{m1}). This is consistent with the inhibitory activity of NO and the lower affinity of O_2 for Cu.

The model was applied to all the data from experiments carried out at low [O_2] (some of which are presented in Fig. 1C and D and Fig. 2A–D). The kinetic parameters thus obtained were used to simulate the experimental traces collected over a 4-fold extended [O_2] range, which are shown in Fig. 5, and to generate the lines in Fig. 3A and B. The experiments in the high-O_2 range were designed to test the predictive ability of the model beyond the range over which the parameters were fitted.

In the minimum model of linear competitive inhibition [22], the apparent inhibition constant, K'_i, determines the proportionality by which the c_{50} (the [O_2] required to achieve half V_{max} at any given [NO]) is increased as a linear function of [NO]. This model fails to explain the non-linear dependence of c_{50} on [NO] that we observed in intact cells (not shown). A more accurate prediction is given by the following equation, derived from our model:

$$c_{50} = \frac{K_{uNO}K_{m1}K_{m2}(K_{icNO} + [NO])}{K_{icNO}K_{uNO}K_{m2} + [NO]K_{uNO}K_{m1} + [NO]K_{icNO}K_{m2}} \quad (3)$$

The IC_{50} is defined as the [NO] that inhibits mitochondrial respiration by 50% relative to flux at the same [O_2] in the absence of NO. In the competitive model, IC_{50} is a linear function of [O_2] [22]; our data in intact cells show that IC_{50} is a non-linear function of [O_2] (Fig. 3B), which our model predicts to be determined as follows:

$$IC_{50} = \frac{K_{uNO}K_{icNO}K_{m2}(K_{m1} + [O_2])}{K_{m1}K_{uNO}K_{m2} + [O_2]K_{m2}K_{icNO} - 2rK_{m1}^2K_{uNO} - (2r-1)[O_2]K_{uNO}K_{m1}} \quad (4)$$

where r represents the ratio V_{max2}/V_{max1}.

We are aware of the limitations of the proposed model, which (i) assumes that the cell's reducing pressure is constant and neglects the reduction steps of the catalytic cycle, and (ii) may attribute to CcO roles played by other components of the cell. These limitations, however, do

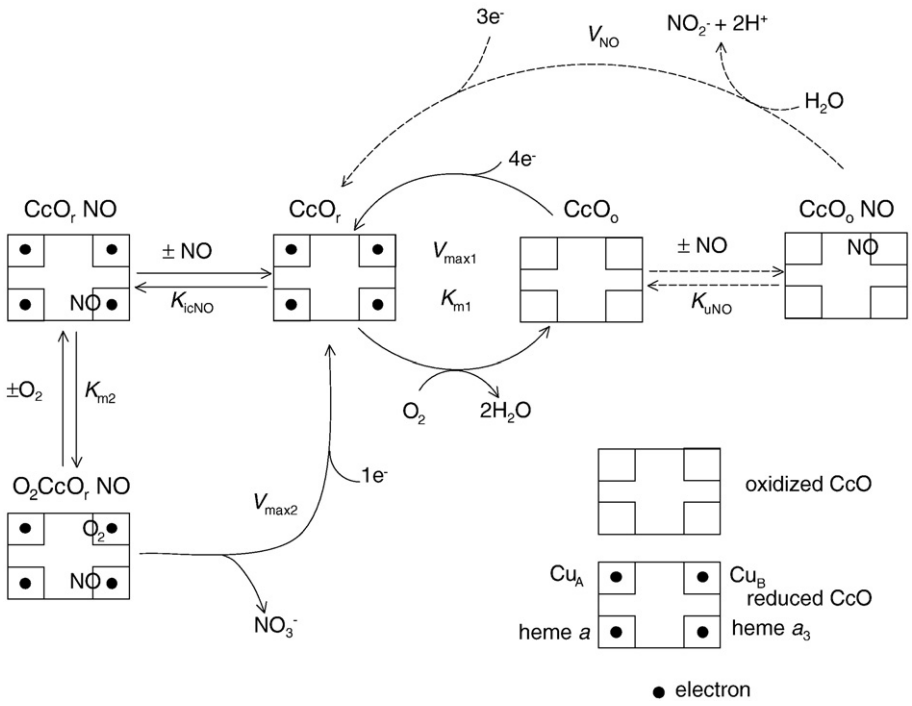

Fig. 4. Scheme representing the proposed model of NO-inhibition of CcO. A simplified catalytic cycle under constant reducing pressure is adopted for CcO in the absence of NO, described by the steady state parameters K_{m1} and V_{max1}. NO is assumed to bind to both the fully reduced and the fully oxidized states of the enzyme, with the dissociation constants K_{icNO} and K_{uNO} respectively. When NO binds to the reduced heme a_3 dissociation can also occur after oxidation of the gas to nitrate ion, thanks to a molecule of O_2 activated by Cu_B (see text and Refs. [45,46]); this goes through a complete alternative catalytic cycle described by the steady state parameters K_{m2} and V_{max2}. NO bound to Cu_B can in turn be oxidized by the metal and be released as nitrite ion (NO_2^-) in a reaction that does not require O_2 (described by V_{NO}). Dashed arrows indicate reactions described in the literature but that occur only to a minimal extent under our experimental conditions and can be safely neglected in the quantitative analysis of our data. CcO_r, reduced CcO; CcO_rNO, CcO_r with NO bound to heme a_3; O_2CcO_rNO, CcO_r with NO bound to heme a_3 and O_2 bound to Cu_B; CcO_o, oxidized CcO; CcO_oNO, CcO_o with NO bound to Cu_B.

not seem to us to be major drawbacks since the aim of the model is to describe cell respiration under NO stress via a chemically sound, though oversimplified, reaction mechanism.

3.5. NO dynamics in the low- and high-O_2 ranges

At high levels of iNOS expression (50 ng/ml tetracycline) NO production in the low-O_2 range is sufficiently fast to reach high, near steady-state NO concentrations of 1.5 μM within 10–15 min, when O_2 drops to 30 μM and becomes limiting for NO production (Fig. 5A and B). In the high-O_2 range, the further increase of [NO] from 10 to 40 min is modest (from 1.5 to 2 μM), indicating a near-balance between NO production and utilization at NO concentrations in the upper pathophysiological range (Fig. 5C and D). In contrast, at low levels of iNOS expression (20 ng/ml tetracycline) in the low-O_2 range, respiration is less inhibited and 30 μM O_2 is reached in less than 5 min (Fig. 5E), at a time when the steep increase in [NO] continues near-linearly at high [O_2] (Fig. 5G). There is an additional period of approximately 40 min in the high-O_2 range, during which net NO production is positive and hence NO accumulates, until again at around 30 μM O_2 the balance shifts to NO degradation and the [NO] level falls (Fig. 5G and H). A plot of critical [O_2] for limitation of NO production, against [NO] is shown in Fig. 6. Although the critical [O_2] is a complex function of iNOS expression levels and O_2 range, it was actually restricted to a surprisingly narrow range under all experimental conditions.

3.6. Reversible inhibition and NO-induced activation of the cellular metabolic state

We performed a series of experiments to study the reversibility of the inhibition. Addition of HbO_2 to cells producing high levels of NO (50 ng/ml tetracycline and 1 mM L-arginine) resulted not only in full recovery but in a significant increase in cellular respiration above the routine reference level observed before L-arginine addition (Fig. 7A). Respiration was also recovered after inhibition of iNOS activity with S-EITU (1 mM; not shown). No irreversible effects were observed up to 1.8 μM NO. Moreover, when the cell suspension was illuminated with a cold light source at 60 μM O_2, the respiration rate immediately increased above the reference level; this reflects the photochemical dissociation of the reduced heme a_3–NO complex [35–37], again revealing the NO-induced stimulation of cell respiration (Fig. 7B). Light had no effect on respiration in the absence of NO (not shown).

We define the stimulation factor, *F*, as the ratio of V_{max1} after NO removal to V_{max1} before L-arginine addition (Fig. 7C). *F* was usually between 1 and 1.5 and we attribute it to the accumulation of reduced cytochrome *c* and a decline in mitochondrial membrane potential caused by CcO inhibition. Stimulation causes V_{max1} (and V_{max2}) to be variable, rather than constant, parameters; however, our model assumes constant reducing pressure and neglects the stimulation effect. Nevertheless, stimulation is significant only at high [NO], where V_{max2} predominates, while at low [NO] the absence of stimulation is associated with predominance of V_{max1}. Therefore the stimulation effect is partially reflected in the ratio of V_{max2} to V_{max1} ($r = V_{max2}/V_{max1}$). A plot of normalized fluxes predicted from the kinetic model plotted against experimentally determined fluxes is depicted in Fig. 7D.

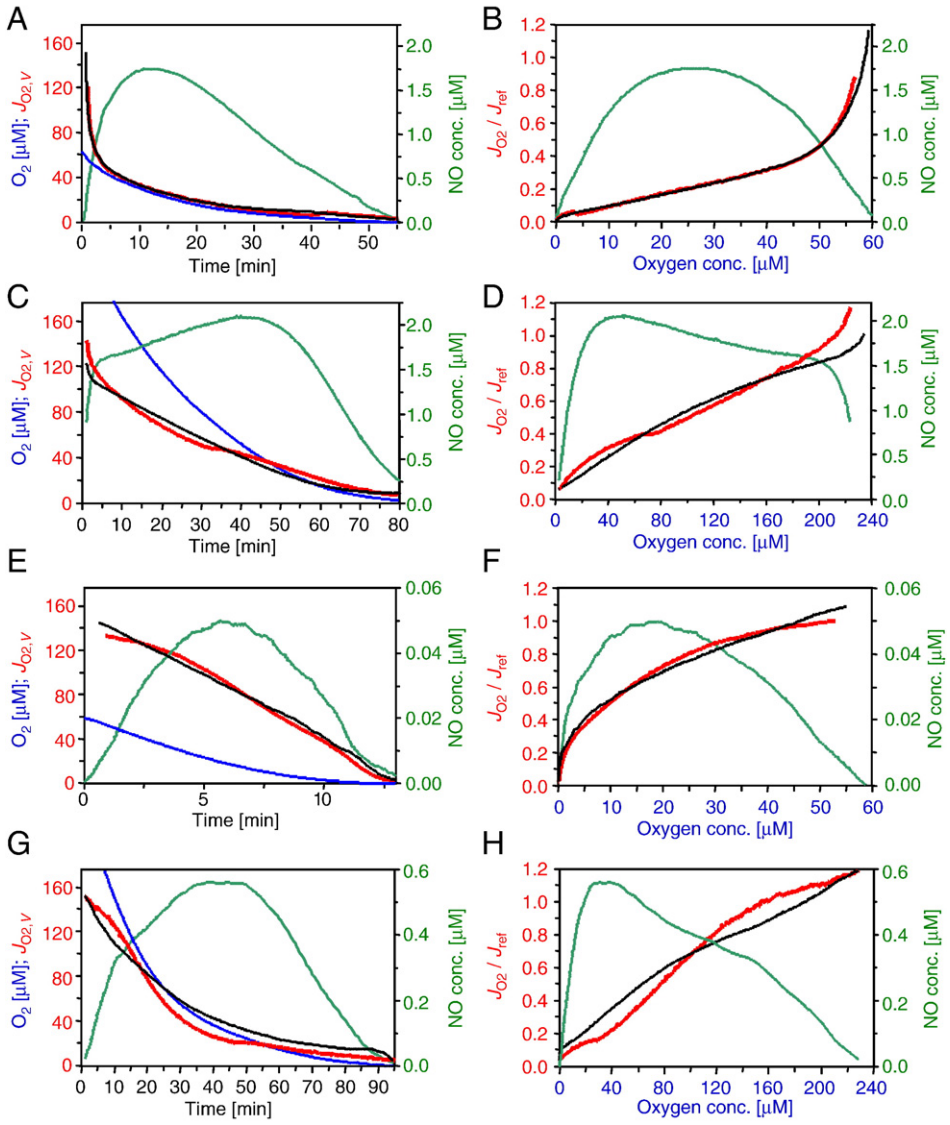

Fig. 5. NO production and NO-induced inhibition of respiration over a standard (A,B,E,F) or extended (C,D,G,H) [O_2] range. O_2 consumption and NO production were measured at high (50 ng/ml tetracycline; A–D) and low (20 ng/ml tetracycline; E–H) iNOS activities. (A,C,E,G) Oxygraph-2k traces of [O_2] (blue), O_2 flux (red) and [NO] (green) as a function of time, with data points plotted at 1 s intervals. (B,D,F,H) Relative measured flux (red), estimated flux from the kinetic model (black) and [NO] (green) as a function of [O_2]. Traces are representative of three similar experiments.

4. Discussion

We present a detailed study of the O_2 kinetics of cellular respiration at varying concentrations of endogenous NO over the pathophysiological range. Based on the results, we propose a kinetic model of NO-induced inhibition of cellular respiration that explains the experimental data and has predictive value. The model assumes that the system can be treated under the pseudo-equilibrium approximation and that two cycles, each characterized by its own K_m and V_{max}, are possible, one for NO-free and one for NO-bound CcO. The pseudo-equilibrium assumption is unrealistic, but greatly simplifies the analysis at the expense of some parameters becoming apparent, rather than real, kinetic constants. The model invokes both competitive inhibition (at the heme a_3 site) and uncompetitive inhibition (at Cu_B), as previously described [25–28]. The details of the complex catalytic cycle of CcO are ignored, in particular in relation to the reduction intermediates. V_{max1} corresponds to routine respiration of the intact cell at saturating [O_2] in the absence of NO. Routine respiration is regulated at a modest level of activity, significantly below the maximum capacity of the electron transport system, and thus below the true V_{max} for CcO [41], as shown by the results listed in Table 1 and by the NO-induced stimulation of respiration (Fig. 7A and B). Notably, increases in [NO] that are unable to inhibit cell respiration reduce CcO, and the excess capacity of the enzyme is able to maintain O_2 consumption in the cell [47].

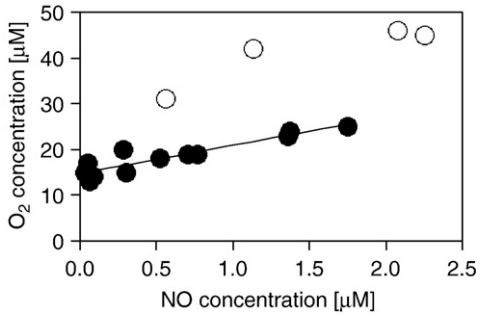

Fig. 6. Critical [O_2] for limitation of NO production. Critical [O_2] for net NO production, below which [NO] declines. High [NO] corresponds to high iNOS activities in the low- and high-O_2 ranges (full and open circles, respectively).

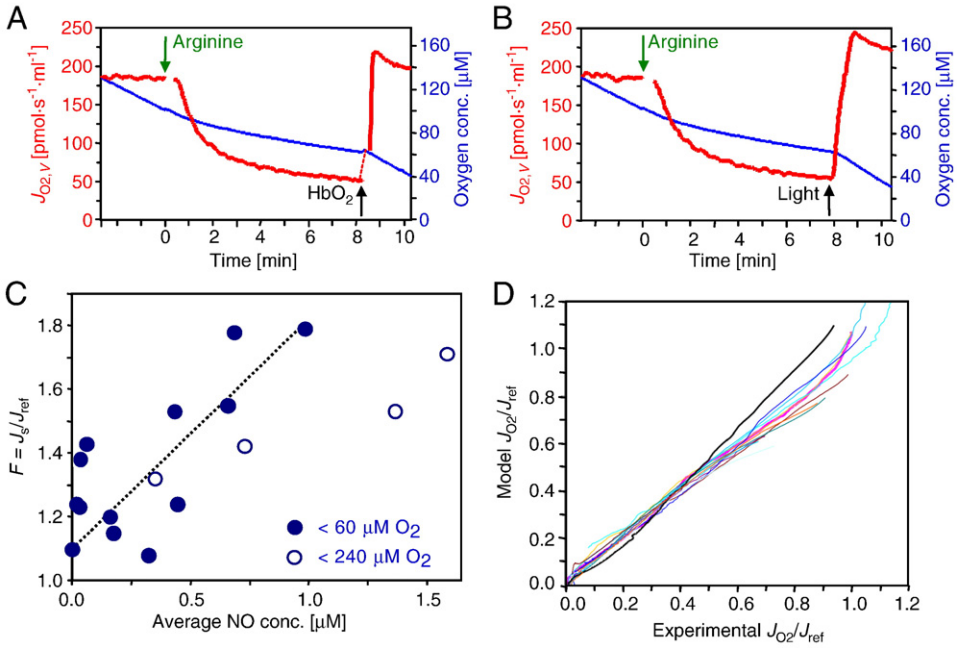

Fig. 7. Stimulation of respiration following NO removal. (A,B) Oxygraph traces of $[O_2]$ (blue) and O_2 flux (red) in cells treated with tetracycline (50 ng/ml), showing the inhibition of respiration induced by the addition of L-arginine (1 mM). Subsequent addition of HbO_2 (A) or illumination with a cold light source (B) stimulated respiration (J_s) above the initial reference level. (C) Stimulation factor ($F = J_s/J_{ref}$) as a function of [NO]. (D) Normalized fluxes predicted from the kinetic model (hyperbolic approximation, see Supporting information) plotted against experimentally determined fluxes.

The model is designed to incorporate two important observations from previous studies on purified CcO or its model compounds. First, it allows NO bound to oxidized CcO to act as a slow reductant, rather than as an inhibitor, by donating its unpaired electron. The resulting nitrosonium ion (NO^+), dissociates *via* conversion to nitrite (NO_2^-) in a non-redox reaction with a water molecule [27,48]. Second, the model includes an NO-dissociation cycle (for the derivative CcO_rNO) that consumes O_2, albeit with a high K_m (K_{m2}). This can account for the low O_2 consumption we observed experimentally at high [NO]. Although this reaction has not been observed unequivocally in isolated CcO, and was not detected in specifically designed experiments [49], it has been suggested by Pearce et al. [45], and has been directly demonstrated for a model compound mimicking the binuclear site of CcO synthesized by Collman et al. [46]. Our data cannot resolve this issue, due to the complexity of the system studied (whole cells, rather than purified CcO). However, we unequivocally observed respiration at NO concentrations that should fully inhibit CcO activity in the absence of a mechanism like the one proposed in Fig. 4 and Refs. [45,46].

Our model fits the experimental data and is compatible with what is known about the interaction between CcO and NO [25,45,46]; however, it may not provide a complete description of the observed O_2 fluxes in intact living cells. Other reactions between O_2 and NO are possible, either spontaneous or catalyzed by cell components other than CcO. These reactions, as well as functions played by other cellular components, would contribute to O_2 consumption and in our model would be wrongly attributed to CcO. Nonetheless, our model provides a chemically sound quantitative description of our data and has predictive value. We also tested a variant model, in which O_2 oxidizes the NO molecule bound to Cu_B, rather than the one bound to heme a_3 [50]. Although this variant accurately fits the experimental data, it was discarded because it lacks independent support; indeed no such reaction was reported for the synthetic model of CcO [46].

The most important feature of the model presented here is that the relative population of the catalytically active species O_2CcO_rNO (represented by the term $[O_2][NO]/K_{m2}K_{icNO}$ in Eq. (1)) is proportional to the product of the concentrations of NO and O_2. This provides an explanation for how the enzyme can be active at relatively high inhibitor concentrations and also explains the non-linear IC_{50} vs. $[O_2]$ plot (Fig. 3B). An IC_{50} vs. $[O_2]$ plot similar to ours was presented by Koivisto et al. [24]; however, these authors proposed that two O_2 molecules need to bind to CcO to compete with NO, which is unlikely. Our hypothesis provides a sounder solution to this problem. More recently, using published data mainly obtained with NO donors, an IC_{50} vs. $[O_2]$ plot similar to ours has been reported [51].

In conclusion, we show the dependence of NO production on $[O_2]$ and the interplay between O_2 and NO concentrations in determining cell respiration. In spite of its complexity, this interplay can be described by a relatively simple and chemically sound kinetic model. The control of respiration by NO regulates O_2 gradients in the cell, redox signaling and apoptosis [52]. Furthermore, interactions of NO with mitochondria have important implications for ischemic biology [33,53] and hypoxic vasodilation [54], and their understanding will help clarify the mechanisms by which NO exerts cardioprotective actions [55].

Acknowledgements

We thank Alessandro Giuffré (Università di Roma 'Sapienza', Italy) for his helpful comments on the paper, Jesús Mateo (CNIC) for the Tet-iNOS 293 cells, Cristina Vaca (Hospital Universitario de La Princesa) for the technical assistance, Chris Cooper (University of Essex, UK) for the helpful discussions and Simon Bartlett (CNIC) for the editorial work. This work was supported by Ministerio de Ciencia e Innovación (MICINN) grant BFI2003-03493 and by Instituto de Salud Carlos III grants PI060701, PS09/00116 and CP08/00204, all to SC. AB acknowledges support from Ateneo Federato PSS of the Università di Roma 'Sapienza'. We also acknowledge the support of an Acciones Integradas grant HU2006-0009 from the MICINN to EG and SC. Predoctoral fellowships from the MICINN were received by EA and FR-J (FPI). SC was funded by the 'Ramón y Cajal' and 'Miguel Servet' programs.

Appendix A. Supplementary data

Supplementary data associated with this article can be found, in the online version, at doi:10.1016/j.bbabio.2010.01.033.

References

[1] B. Roy, J. Garthwaite, Nitric oxide activation of guanylyl cyclase in cells revisited, Proc. Natl. Acad. Sci. U. S. A. 103 (2006) 12185–12190.
[2] J. Schlossmann, F. Hofmann, cGMP-dependent protein kinases in drug discovery, Drug Discov. Today 10 (2005) 627–634.
[3] G.C. Brown, C.E. Cooper, Nanomolar concentrations of nitric oxide reversibly inhibit synaptosomal respiration by competing with oxygen at cytochrome oxidase, FEBS Lett. 356 (1994) 295–298.
[4] M.W. Cleeter, J.M. Cooper, V.M. Darley-Usmar, S. Moncada, A.H. Schapira, Reversible inhibition of cytochrome *c* oxidase, the terminal enzyme of the mitochondrial respiratory chain, by nitric oxide. Implications for neurodegenerative diseases, FEBS Lett. 345 (1994) 50–54.
[5] M. Schweizer, C. Richter, Nitric oxide potently and reversibly de-energizes mitochondria at low oxygen tension, Biochem. Biophys. Res. Commun. 204 (1994) 169–175.
[6] G.C. Brown, Nitric oxide regulates mitochondrial respiration and cell functions by inhibiting cytochrome oxidase, FEBS Lett. 369 (1995) 136–139.
[7] C.E. Cooper, Nitric oxide and cytochrome oxidase: substrate, inhibitor or effector? Trends Biochem. Sci. 27 (2002) 33–39.
[8] E. Clementi, G.C. Brown, N. Foxwell, S. Moncada, On the mechanism by which vascular endothelial cells regulate their oxygen consumption, Proc. Natl. Acad. Sci. U. S. A. 96 (1999) 1559–1562.
[9] S. Moncada, J.D. Erusalimsky, Does nitric oxide modulate mitochondrial energy generation and apoptosis? Nat. Rev. Mol. Cell Biol. 3 (2002) 214–220.
[10] P.S. Brookes, D.W. Krauss, S. Shiva, J.E. Doeller, M.C. Barone, R.P. Patel, J.R. Lancaster Jr., V. Darley-Usmar, Control of mitochondrial respiration by NO, effects of low oxygen and respiratory state, J. Biol. Chem. 278 (2003) 31603–31609.
[11] M. Palacios-Callender, M. Quintero, V.S. Hollis, R.J. Springett, S. Moncada, Endogenous NO regulates superoxide production at low oxygen concentrations by modifying the redox state of cytochrome *c* oxidase, Proc. Natl. Acad. Sci. USA 101 (2004) 7630–7635.
[12] P. Brookes, V.M. Darley-Usmar, Hypothesis: the mitochondrial NO signalling pathway, and the transduction of nitrosative to oxidative cell signals: an alternative function for cytochrome *c* oxidase, Free Radic. Biol. Med. 32 (2002) 370–374.
[13] T. Hagen, T.C. Taylor, F. Lam, S. Moncada, Redistribution of intracellular oxygen in hypoxia by nitric oxide: effect on HIF1alpha, Science 302 (2003) 1975–1978.
[14] A. Almeida, S. Moncada, J.P. Bolaños, Nitric oxide switches on glycolysis through the AMP protein kinase and 6-phosphofructo-2-kinase pathway, Nat. Cell Biol. 6 (2004) 45–51.
[15] D.D. Thomas, X. Liu, S.P. Kantrow, J.R. Lancaster Jr., The biological lifetime of nitric oxide: implications for the perivascular dynamics of NO and O_2, Proc. Natl. Acad. Sci. U. S. A. 98 (2001) 355–360.
[16] W. Xu, L. Liu, I.G. Charles, S. Moncada, Nitric oxide induces coupling of mitochondrial signalling with the endoplasmic reticulum stress response, Nat. Cell Biol. 6 (2004) 1129–1134.
[17] A. Gjedde, P. Johannsen, G.E. Cold, L. Østergaard, Cerebral metabolic response to low blood flow: possible role of cytochrome oxidase inhibition, J. Cereb. Blod Flow Metab. 25 (2005) 1183–1196.
[18] D. Brealey, M. Brand, I. Hargreaves, S. Heales, J. Land, R. Smolenski, N.A. Davies, C.E. Cooper, M. Singer, Association between mitochondrial dysfunction and severity and outcome of septic shock, Lancet 360 (2002) 219–223.
[19] S. Moncada, J.P. Bolaños, Nitric oxide, cell bioenergetics and neurodegeneration, J. Neurochem. 97 (2006) 1676–1689.
[20] P. Sarti, A. Giuffrè, M.C. Barone, E. Forte, D. Mastronicola, M. Brunori, Nitric oxide and cytochrome oxidase: reaction mechanisms from the enzyme to the cell, Free Radic. Biol. Med. 34 (2003) 509–520.
[21] F. Malatesta, G. Antonini, P. Sarti, M. Brunori, Structure and function of a molecular machine: cytochrome *c* oxidase, Biophys. Chem. 54 (1995) 1–33.
[22] F. Antunes, A. Boveris, E. Cadenas, On the mechanism and biology of cytochrome oxidase inhibition by nitric oxide, Proc. Natl. Acad. Sci. U. S. A. 101 (2004) 16774–16779.
[23] T.C. Bellamy, C. Griffiths, J. Garthwaite, Differential sensitivity of guanylyl cyclase and mitochondrial respiration to nitric oxide measured using clamped concentrations, J. Biol. Chem. 277 (2002) 31801–31807.
[24] A. Koivisto, A. Matthias, G. Bronnikov, J. Nedergaard, Kinetics of the inhibition of mitochondrial respiration by NO, FEBS Lett. 417 (1997) 75–80.
[25] M.G. Mason, P. Nicholls, M.T. Wilson, C.E. Cooper, Nitric oxide inhibition of respiration involves both competitive (heme) and non-competitive (copper) binding to cytochrome *c* oxidase, Proc. Natl. Acad. Sci. U. S. A. 103 (2006) 708–713.
[26] M. Brunori, E. Forte, M. Arese, D. Mastronicola, A. Giuffrè, P. Sarti, Nitric oxide and the respiratory enzyme, Biochim. Biophys. Acta 1757 (2006) 1144–1154.
[27] F. Antunes, A. Boveris, E. Cadenas, On the biologic role of the reaction of NO with oxidized cytochrome *c* oxidase, Antioxid. Redox Signal. 9 (2007) 1569–1579.
[28] C.E. Cooper, M.G. Mason, P. Nicholls, A dynamic model of nitric oxide inhibition of mitochondrial cytochrome *c* oxidase, Biochim. Biophys. Acta 1777 (2008) 867–876.
[29] D. Mastronicola, M.L. Genova, M. Arese, M.C. Barone, A. Giuffrè, C. Bianchi, M. Brunori, G. Lenaz, P. Sarti, Control of respiration by nitric oxide in Keilin–Hartree particles, mitochondria and SH-SY5Y neuroblastoma cells, Cell. Mol. Life Sci. 60 (2003) 1752–1759.
[30] C.E. Cooper, N.A. Davies, M. Psychoulis, L. Canevari, T.E. Bates, M.S. Dobbie, C.S. Casley, M.A. Sharpe, Nitric oxide and peroxynitrite cause irreversible increases in the K_m for oxygen of mitochondrial cytochrome oxidase: in vitro and in vivo studies, Biochim. Biophys. Acta 1607 (2003) 27–34.
[31] E. Gnaiger, Bioenergetics at low oxygen: dependence of respiration and phosphorylation on oxygen and adenosine diphosphate supply, Respir. Physiol. 128 (2001) 277–297.
[32] J. Mateo, M. García-Lecea, S. Cadenas, C. Hernández, S. Moncada, Regulation of hypoxia inducible factor-1α by nitric oxide through mitochondria-dependent and -independent pathways, Biochem. J. 376 (2003) 537–544.
[33] F. Rodríguez-Juárez, E. Aguirre, S. Cadenas, Relative sensitivity of soluble guanylate cyclase and mitochondrial respiration to endogenous nitric oxide at physiological oxygen concentration, Biochem. J. 405 (2007) 223–231.
[34] E. Gnaiger, Oxygen conformance of cellular respiration. A perspective of mitochondrial physiology, Adv. Exp. Med. Biol. 543 (2003) 39–55.
[35] R. Boelens, R. Wever, B.F. Van Gelder, H. Rademaker, An EPR study of the photodissociation reactions of oxidised cytochrome *c* oxidase–nitric oxide complexes, Biochim. Biophys. Acta 724 (1983) 176–183.
[36] P. Sarti, A. Giuffrè, E. Forte, D. Mastronicola, M.C. Barone, M. Brunori, Nitric oxide and cytochrome *c* oxidase: mechanisms of inhibition and NO degradation, Biochem. Biophys. Res. Commun. 274 (2000) 183–187.
[37] V. Borutaite, A. Budriunaite, G.C. Brown, Reversal of nitric oxide-, peroxynitrite- and *S*-nitrosothiol-induced inhibition of mitochondrial respiration or complex I activity by light and thiols, Biochim. Biophys. Acta 1459 (2002) 405–412.
[38] A. Rengasamy, R.A. Johns, Determination of K_m for oxygen of nitric oxide synthase isoforms, J. Pharmacol. Exp. Ther. 276 (1996) 30–33.
[39] J. Santolini, A.L. Meade, D.J. Stuehr, Differences in three kinetic parameters underpin the unique catalytic profiles of nitric-oxide synthases I, II and III, J. Biol. Chem. 276 (2001) 48887–48898.
[40] E. Gnaiger, G. Mendez, S.C. Hand, High phosphorylation efficiency and depression of uncoupled respiration in mitochondria under hypoxia, Proc. Natl. Acad. Sci. U. S. A. 97 (2000) 11080–11085.
[41] E. Gnaiger, B. Lassnig, A.V. Kuznetsov, G. Rieger, R. Margreiter, Mitochondrial oxygen affinity, respiratory flux control, and excess capacity of cytochrome *c* oxidase, J. Exp. Biol. 201 (1998) 1129–1139.
[42] P. Pecina, E. Gnaiger, J. Zeman, E. Pronicka, J. Houstek, Decreased affinity for oxygen of cytochrome-c oxidase in Leigh syndrome caused by SURF1 mutations, Am. J. Physiol. Cell Physiol. 287 (2004) C1384–C1388.
[43] E. Gnaiger, B. Lassnig, A.V. Kuznetsov, R. Margreiter, Mitochondrial respiration in the low oxygen environment of the cell. Effect of ADP on oxygen kinetics, Biochim. Biophys. Acta 1365 (1998) 249–254.
[44] P.R. Castello, P.S. David, T. McClure, Z. Crook, R.O. Poyton, Mitochondrial cytochrome oxidase produces nitric oxide under hypoxic conditions: implications for oxygen sensing and hypoxic signaling in eukaryotes, Cell Metab. 3 (2006) 277–287.
[45] L.L. Pearce, A.J. Kanai, L.A. Birder, B.R. Pitt, J. Peterson, The catabolic fate of nitric oxide. The nitric oxide oxidase and peroxynitrite reductase activities of cytochrome oxidase, J. Biol. Chem. 277 (2002) 13556–13562.
[46] J.P. Collman, A. Dey, R.A. Decreau, Y. Yang, A. Hosseini, E.I. Solomon, T.A. Eberspacher, Interaction of nitric oxide with a functional model of cytochrome *c* oxidase, Proc. Natl. Acad. Sci. U. S. A. 105 (2008) 9892–9896.
[47] M. Palacios-Callender, V. Hollis, N. Frakich, J. Mateo, S. Moncada, Cytochrome *c* oxidase maintains mitochondrial respiration during partial inhibition by nitric oxide, J. Cell Sci. 120 (2007) 160–165.
[48] J. Torres, M.A. Sharpe, A. Rosquist, C.E. Cooper, M.T. Wilson, Cytochrome *c* oxidase rapidly metabolises nitric oxide to nitrite, FEBS Lett. 475 (2000) 263–266.
[49] A. Giuffre, E. Forte, M. Brunori, P. Sarti, Nitric oxide, cytochrome *c* oxidase and myoglobin: competition and reaction pathways, FEBS Lett. 579 (2005) 2528–2532.
[50] S. Cadenas, E. Aguirre, F. Rodríguez-Juárez, A. Bellelli, G. Gnaiger, Kinetic model of nitric oxide inhibition of cellular respiration in intact cells, Biochim. Biophys. Acta 1777 (2008) S60 EBEC Abstract Suppl.
[51] C.N. Hall, D. Attwell, Assessing the physiological concentration and targets of nitric oxide in brain tissue, J. Physiol. 586 (2008) 3597–3615.
[52] S. Shiva, V.M. Darley-Usmar, Control of the nitric oxide-cytochrome *c* oxidase signalling pathway under pathological and physiological conditions, IUBMB Life 55 (2003) 585–590.
[53] S. Shiva, P.S. Brookes, R.P. Patel, P.G. Anderson, V.M. Darley-Usmar, Nitric oxide partitioning into mitochondrial membranes and the control of respiration at cytochrome *c* oxidase, Proc. Natl. Acad. Sci. U. S. A. 98 (2001) 7212–7217.
[54] M. Palacios-Callender, V. Hollis, M. Mitchison, N. Frakich, D. Unitt, S. Moncada, Cytochrome *c* oxidase regulates endogenous nitric oxide availability in respiring cells: a possible explanation for hypoxic vasodilation, Proc. Natl. Acad. Sci. U. S. A. 104 (2007) 18508–18513.
[55] S.P. Jones, R. Bolli, The ubiquitous role of nitric oxide in cardioprotection, J. Mol. Cell. Cardiol. 40 (2006) 16–23.